The Cryosphere Discuss., 8, 1453–1477, 2014
www.the-cryosphere-discuss.net/8/1453/2014/
doi:10.5194/tcd-8-1453-2014

The Cryosphere
Discussions
Open Access

Small impact of surrounding oceanic conditions on 2007–2012 Greenland Ice Sheet surface mass balance

B. Noël[1,2], X. Fettweis[1], W. J. van de Berg[2], M. R. van den Broeke[2], and M. Erpicum[1]

[1]Department of Geography, University of Liège, Belgium
[2]Institute for Marine and Atmospheric research Utrecht, University of Utrecht, the Netherlands

Received: 31 January 2014 – Accepted: 14 February 2014 – Published: 4 March 2014

Correspondence to: B. Noël (B.P.Y.Noel@uu.nl)

Published by Copernicus Publications on behalf of the European Geosciences Union.

Abstract

During recent summers (2007–2012), several surface melt records were broken over the Greenland Ice Sheet (GrIS). The extreme summer melt resulted in part from a persistent negative phase of the North-Atlantic Oscillation (NAO), favouring warmer than normal conditions over the GrIS. In addition, it has been suggested that significant anomalies in sea ice cover (SIC) and sea surface temperature (SST) may partially explain recent anomalous GrIS surface melt. To assess the impact of 2007–2012 SIC and SST anomalies on GrIS surface mass balance (SMB), a set of sensitivity experiments was carried out with the regional climate model MAR. These simulations suggest that changes in SST and SIC in the seas surrounding Greenland do not significantly impact GrIS SMB, due to the katabatic winds blocking effect. These winds are strong enough to prevent oceanic near-surface air, influenced by SIC and SST variability, from penetrating far inland. Therefore, the ice sheet SMB response is restricted to coastal regions, where katabatic winds are weaker. However, anomalies in SIC and SST could have indirectly affected the surface melt by changing the general circulation in the North Atlantic region, favouring more frequent warm air advection to the GrIS.

1 Introduction

With an area of ≈ 1.7 million km^2, covering more than 80 % of Greenland, the Greenland Ice Sheet (GrIS) is the world's second largest ice sheet. The GrIS contains almost 10 % of the Earth's total fresh water, equivalent to ≈ 7 m of global mean sea level rise. The ice sheet thickness is about 3 km at its centre and progressively decreases towards the ice-free tundra regions (Hanna et al., 2009). Previous work has shown that the GrIS is strongly sensitive to climate warming; in response to a combination of natural and anthropogenic forcings, its mass loss has accelerated over the last decades (Rignot et al., 2011; Enderlin and Howat, 2013; Fettweis et al., 2013b; Wouters et al., 2013). Enhanced surface melting and iceberg calving make that the GrIS contributes

TCD
8, 1453–1477, 2014

significantly (≈ 25 %) to ongoing global sea level rise, affecting coastal regions worldwide. Moreover, by increasing the discharge of fresh meltwater into the Atlantic Ocean and lowering its salinity, GrIS mass loss has the potential to weaken the Atlantic thermohaline circulation (Hanna et al., 2009), partly mitigating projected climate warming in north-western Europe. Since 2007, several melt records were broken over the GrIS (Hanna et al., 2013a). For instance, July 2012 was characterized by the largest melt extent ever recorded during the satellite era, affecting 97 % of the ice sheet surface (Tedesco et al., 2013).

To explain these events, several hypotheses have been put forward in recent studies. Oceanic forcing, i.e. changes in sea ice cover (SIC) and sea surface temperature (SST) of the oceans surrounding Greenland, could have contributed to GrIS SMB decline by increasing near-surface air temperature over and moisture advection towards the ice sheet. In previous studies, the influence of oceanic forcing on GrIS SMB was estimated from model sensitivity experiments, for instance, using the regional climate model MAR (Modèle Atmosphérique Régional) forced by ERA-Interim reanalyses, based on imposing SST variations (Hanna et al., 2009) or a combination of SIC-SST variations (Hanna et al., 2013a). The first experiment suggested that SST variations (±2 °C) alone can not fully explain the GrIS melt record observed in the summer of 2007 (Hanna et al., 2009). In the second experiment, Hanna et al. (2013a) used the climatological mean SST and SIC over 1979–1994 to prescribe oceanic conditions in MAR, instead of the values observed in 2012. They showed that this combination of SIC and SST anomalies again did not significantly influence GrIS SMB observed in the summer of 2012. Furthermore, Day et al. (2013) carried out 2 sensitivity experiments, consisting of a SIC reduction and a combination of a decrease in SIC and increase in SST, to determine the impact of oceanic forcings on GrIS SMB over a 30 year period. In this study, they used the regional climate model HadRM3, forced every 6 h by the global circulation model HadAM3. In addition, monthly mean SIC and SST, averaged over 2061–2090 and based on the A1B scenario, were used to force HadRM3 and HadAM3. The comparison with a reference run, characterized by present-day SST and monthly mean SIC over 1961–1990, allowed Day et al. (2013) to isolate the effect of SIC and combined SIC-SST anomalies on GrIS SMB. The results suggest that the SIC reduction alone leads to a winter precipitation increase, spatially restricted to the centre and eastern parts of the GrIS, and resulting from stronger evaporation over the ice-free ocean. During summer, a SIC decrease weakens North Atlantic cyclonic activity, lowering precipitation over the southern GrIS (Hoskins and Hodges, 2002; Day et al., 2013). The higher winter precipitation increases surface albedo, reducing the summer runoff and resulting in a positive SMB anomaly. The results of the combined SIC-SST forcing shows that a warmer and wetter atmosphere tends to increase precipitation over the GrIS. However, this mass gain is exceeded by enhanced runoff, leading to a net decrease in SMB (Day et al., 2013).

Anomalous atmospheric forcing, specifically the persistent 2007–2012 negative phase of the North Atlantic Oscillation Index (NAOI) in summer, has favoured warmer and drier conditions over the ice sheet, enhancing the melting (Fettweis et al., 2013b). According to Fettweis et al. (2013b), about 70 % of the recent surface melt increase can be attributed to anomalous warm air advection towards the western GrIS (Box et al., 2012). The remaining 30 % is then explained by long-term anthropogenic warming in the Arctic (Fettweis et al., 2013b). However, Hanna et al. (2013b) suggested that the anomalous NAO phase could also result from changes in oceanic forcing (Overland and Wang, 2010; Jaiser et al., 2012). Therefore, oceanic forcing could be responsible for the recent large-scale circulation changes, indirectly impacting GrIS SMB.

In spite of these previous studies, large uncertainties remain in the direct oceanic forcing's impact on GrIS SMB. In their experiments, Hanna et al. (2009, 2013a) used a small integration domain, including only a narrow band of oceanic pixels surrounding the GrIS. If oceanic pixels are close to the regional model domain edges, they will be strongly affected by the lateral boundary forcings, biasing the oceanic impact on the air masses. In addition, both studies only analysed a single year, prescribing oceanic anomalies from May to September. The HadRM3 model, used in Day et al. (2013), is known to significantly underestimate total precipitation and overestimate runoff. Moreover, monthly means of SIC and SST were prescribed in HadRM3 instead of preferred 6 hourly anomalies. Finally, the forcings in these previously published sensitivity experiments might be too weak to generate a significant impact on GrIS SMB.

The aim of this study is to determine whether isolated or coupled SIC and SST anomalies could significantly affect GrIS SMB by prescribing more extreme forcings. Simulations are carried out using MAR forcing at 40 km spatial resolution with a larger domain size than in Hanna et al. (2009, 2013a). MAR has small contemporary biases because it has been especially developed to simulate GrIS SMB (Fettweis, 2007). Furthermore, our sensitivity experiments are not limited to the melting season, using 6 hourly anomalies in SIC and SST prescribed from ERA-Interim for 2007–2012, instead of fixed monthly mean values.

In Sect. 2, the MAR model is briefly introduced as well as the reference and sensitivity simulations. Section 3 describes the impacts of SIC and/or SST anomalies on GrIS SMB. The impact of oceanic forcings on the katabatic wind intensity is discussed in Sect. 4, followed by conclusions in Sect. 5.

2 Model and set-up

2.1 The regional climate model MAR

The MAR model consists of a 3-D coupled atmosphere-land surface model that estimates the evolution of the coupled land-atmosphere system resulting from radiative and atmospheric forcings within the integration domain boundaries (Gallée and Schayes, 1994). MAR is coupled to the 1-D module SISVAT (Soil Ice Snow Vegetation Atmosphere Transfer) (Gallée and Schayes, 1994; Ridder and Gallée, 1998), which simulates mass and energy fluxes between the surface-vegetation-atmosphere system (Tedesco et al., 2013). SISVAT includes a 1-D multi-layered snow model, based on the CEN (Centre d'Etudes de la Neige) snow model CROCUS (Brun et al., 1992), which computes the energy fluxes between the sea ice, the ice sheet surface, the snow-covered tundra and the atmosphere (Gallée et al., 2001; Fettweis, 2007). CROCUS consists of a thermodynamic and water balance module taking into account meltwater refreezing, a snow metamorphism module, a snow/ice discretization module and an integrated surface albedo module (Brun et al., 1992; Gallée et al., 2001). Drifting snow is not taken into account as its variability is assumed to have a small effect on SMB relative to other components (Lenaerts et al., 2012).

MAR's ability to simulate GrIS SMB was demonstrated by comparing MAR outputs (Fettweis, 2007) with in-situ measurements (Lefebre et al., 2003, 2005; Gallée et al., 2005) and satellite observations (Fettweis et al., 2005, 2011; Tedesco and Fettweis, 2012). By simulating GrIS SMB using different spatial resolutions ranging from 15 to 50 km over 1990–2010, Franco et al. (2012) showed that spatial resolution does not have a significant impact on the modelled SMB. This research is based on MAR version 2 (MARv2) and set-ups used in Fettweis et al. (2013b).

2.2 Set-up of MAR simulations

ERA-Interim reanalysis data (Stark et al., 2007; Dee et al., 2011) are used to force MAR at its lateral boundaries every 6 h over 2007–2012. The reanalysis is available at a $0.75^{\circ} \times 0.75^{\circ}$ spatial resolution.

Because MAR is not coupled to an ocean model, ERA-Interim is also used to prescribe the oceanic surface conditions in MAR, i.e. SIC and SST, every 6 h. The ice sheet topography, based on Bamber et al. (2013), is kept fixed; contemporary climate simulations show that ice sheet topography changes are small (Fettweis et al., 2013a).

The integration domain, shown in Fig. 1, extends ≈ 900 km around the GrIS margins (a) to include the neighbouring sea ice and oceans and (b) to avoid direct influence of lateral forcing on simulated GrIS SMB.

TCD
8, 1453–1477, 2014

2.3 Reference run and sensitivity experiments

The reference simulation covers the period 2002–2012. The five first years were used to spin-up the snow model and only outputs over 2007–2012 are considered. ERA-Interim 6 hourly SIC and SST fields are prescribed in MAR for the reference simulation (Fig. 1a and d). The atmospheric boundary conditions are also from ERA-Interim and identical in each sensitivity experiment.

2.3.1 SIC anomaly forcing

In these sensitivity experiments, 6 hourly SIC of each oceanic grid cell, prescribed from ERA-Interim over 2007–2012, is replaced by the maximum (resp. minimum) SIC value from a distance range of 3 to 6 grid cells surrounding the current one. As a result, SIC is progressively increased (resp. decreased) in 3 or 6 peripheral grid cells, i.e. by 120 or 240 km, extending outward/inward from the sea ice boundary. This method avoids abrupt and hence unrealistic changes in the SIC values between adjacent ice-free and sea ice oceanic grid cells (Fig. 1b and c). These experiments are called SIC ±3 and SIC ±6 in the following sections.

To avoid sea ice having a surface temperature (ST) higher than the melting point (0 °C) and open-water having a ST lower than the assumed salt water freezing point (–3 °C), a ST correction is applied to each pixel subjected to SIC change computed as:

$$\mathrm{ST}'_{(i,j)} = \mathrm{SIC}_{(i,j)} \cdot \min(\mathrm{ST}_{\mathrm{melting}}, \mathrm{ST}_{(i,j)}) + (1 - \mathrm{SIC}_{(i,j)}) \cdot \max(\mathrm{ST}_{\mathrm{freezing}}, \mathrm{ST}_{(i,j)})$$

where $\mathrm{ST}'_{(i,j)}$ is the corrected surface temperature in °C for the pixel (i,j); $\mathrm{SIC}_{(i,j)}$ is the new computed SIC of the pixel (i,j); $\mathrm{ST}_{(i,j)}$ is the pixel (i,j) uncorrected surface temperature in °C; $\mathrm{ST}_{\mathrm{melting}}$ is the melting point (0 °C) while $\mathrm{ST}_{\mathrm{freezing}}$ is the salt water freezing point (–3 °C).

TCD
8, 1453–1477, 2014

2.3.2 SST anomaly forcing

For the SST experiments, 6 hourly SST, prescribed by ERA-Interim over 2007–2012, is increased (resp. decreased) by 2 or 4 °C over the ice-free ocean (Fig. 1e and f). These experiments are called SST ±2 and SST ±4 hereafter. For a SST reduction, ice-free oceanic grid cells are converted into ice covered grid cells when ST becomes lower than the assumed salt water freezing point (–3 °C). For sea ice covered grid cells, the ST is limited to the melting point (0 °C) to prevent any SIC change.

2.3.3 Coupled SIC-SST anomaly forcing

For the coupled experiments, an increase (resp. decrease) in SIC is associated with a decrease (resp. increase) in SST to take the sea ice insulation feedback into account. Both 6 hourly SIC and SST changes are computed according to Sects. 2.3.1 and 2.3.2, respectively. These experiments are called SIC ±3/SST ∓2 and SIC ±6/SST ∓4 in the following sections.

Note that the SST and SIC anomalies, prescribed in the sensitivity experiments, have the same order of magnitude as the anomalies observed in 2012 with respect to the 1979–2012 mean (Table 1). To obtain oceanic conditions close to the summer climatological mean, SST −2 and SIC +6 should be applied to summer 2012.

3 Results

Hereafter, only changes in precipitation and runoff are discussed, since these components are the main drivers of GrIS SMB variability (Box et al., 2004).

3.1 SIC sensitivity experiments

An increase in SIC surrounding the GrIS and the associated reduced evaporation over the north Atlantic induces a negative snowfall anomaly that is mainly restricted to the south-eastern GrIS, where precipitation peaks (Fig. S1a, b, see Supplement). No significant changes in rainfall, runoff and melting are simulated (Table 2). For the SIC +6 experiment, the wintertime near-surface temperature decreases by up to 10 °C over the newly sea ice-covered areas, resulting from a sensible heat flux reduction. However, the increase in SIC does not significantly impact runoff, since SST is already close to the melting point (0 °C) along the sea ice edges. This shows that SIC behaves as a heat and moisture insulator over the ocean, mainly impacting winter sensible heat exchange and evaporation, and has a weak influence on summer air temperature, resulting in unchanged runoff over the GrIS (Fig. S2b and e). The greater the sea ice extent anomaly, the sharper the negative anomaly in annual SMB over 2007–2012 (Fig. 2b). Opposite results are shown for a SIC reduction in Fig. 2e.

3.2 SST sensitivity experiments

Higher SSTs induce an increase in evaporation leading to enhanced snowfall (Fig. S1f) and rainfall (Fig. S3f) over the coastal south-eastern GrIS. In addition, positive SST anomalies also partially turn snowfall into rainfall over the southern GrIS, reducing snowfall and the surface albedo especially in summer (Table 2). This impacts surface melting through the positive melt-albedo feedback. Enhanced runoff is also simulated over the GrIS ablation zone as a result of higher near-surface temperatures (Fig. S2f).

Integrated over the GrIS, the mass loss, induced by enhanced runoff, exceeds the mass gain, resulting from increased precipitation (Table 2). This leads to a negative SMB anomaly (Fig. 2f). Opposite results are simulated for a reduction in SST (Fig. 2c).

3.3 Coupled sensitivity experiments

With a combined decrease in SIC and rise in SST, the positive snowfall anomaly is enhanced (Table 2 and Fig. S1g), because both forcings favour enhanced evaporation above the northern Atlantic Ocean. Changes in rainfall and runoff (Figs. S3 and S2d and g) are similar to the changes induced by the increase in SST alone (Figs. S3 and

TCD
8, 1453–1477, 2014

S2c and f), because SIC changes do not significantly affect the air temperature in summer. For the SIC +6/SST −4 experiment, the decline in runoff is smaller than for the SST −4 experiment (Table 2), because increased SIC only decreases the snowfall. This results from the weakened SST influence on near-surface air temperature when SIC expands, highlighting the importance of winter accumulation on summer melt through the surface albedo (Box et al., 2012). The reduction of summer snowfall is quite similar to that simulated for the SST +4 experiment, because SIC anomalies do not significantly influence summer snowfall (Table 2).

For a coupled increase in SIC and decrease in SST, the mass loss resulting from snowfall reduction, and the mass gain due to decreased runoff, are similar in magnitude when integrated over the GrIS (Fig. 2d). Opposite results are simulated for the SIC −6/SST +4 experiment as shown in Fig. 2g. As a result, SMB changes for this coupled experiment are smaller than the changes from the individual sensitivity experiments (Table 2), leaving SMB almost unchanged. This highlights the importance of accurately simulating the snowfall/runoff ratio since changes in these components tend to compensate each other.

4 Discussion

None of the sensitivity experiments suggests a direct significant SST or/and SIC impact on GrIS SMB over 2007–2012 (Table 2). While SMB varies linearly with individual perturbations in SIC and SST, a nonlinear relationship between the combined SIC-SST and SMB is simulated due to compensating effects. The largest SMB anomalies are ±7 % for the two most extreme SIC perturbations (Table 2), which is well within the model SMB uncertainty (Fettweis, 2007). Furthermore, SMB anomalies are mostly restricted to the western coastal regions, driven by runoff changes, and the southeastern region, driven by snowfall changes (Fig. 2).

TCD
8, 1453–1477, 2014

4.1 Katabatic winds blocking effect

An important role in limiting the oceanic forcing impact on GrIS SMB is played by katabatic winds. Katabatic winds represent negatively buoyant air (van Angelen et al., 2013), flowing down from the GrIS summit towards the ocean. As they are directed offshore, katabatic winds prevent near-surface oceanic air, influenced by SIC or/and SST perturbations, from penetrating far onto the GrIS and from significantly affecting its SMB (Fig. 3). As the surface slope decreases over the tundra and surrounding oceans, katabatic winds cease, allowing some oceanic influence on the SMB in coastal regions. The western Greenland coast is more sensitive to oceanic forcing than the eastern coast (Fig. 3) where steeper slopes lead to stronger katabatic winds (Bamber et al., 2001). Moreover, because the impact of changes in SIC and SST on the overlying air is mainly restricted to the atmospheric boundary layer (Fig. 3), heat and moisture advection in the free atmosphere is not significantly affected by changes in near-surface air over the ocean, but is rather driven by the prescribed boundary conditions.

Oceanic forcing impact on GrIS SMB is enhanced in summer, when katabatic winds weaken (Fig. 3a) in agreement with Rennermalm et al. (2009); Ettema et al. (2010) and van Angelen et al. (2013).

4.2 Oceanic forcing impacts on katabatic winds speed

Since sea ice does not affect near-surface temperature in summer, changes in SIC do not have a significant impact on the June-July-August (JJA) thermal gradient between the ice sheet and the ocean (Fig. S4b and e), leading to insignificant changes in katabatic wind intensity (Fig. 4b and e). In winter, a SIC decrease leads to a sharp rise in near-surface temperature, generating a surface pressure reduction over the oceanic areas affected by a sea ice withdrawal (Fig. S5e). This leads to a small and insignificant enhancement of winter katabatic flow (Fig. 5e).

Horizontal temperature gradient increases with rising ocean temperatures (Figs. S4 and S5f), resulting in enhanced katabatic winds speed over coastal regions (Figs. 4

and 5f). However, changes in surface conditions are less extensive in winter than in summer as the SST anomalies are restricted to ice-free oceanic areas. Significant katabatic wind intensity enhancement, induced by a warmer ocean, is therefore limited to the summer season (Fig. 4f).

Similar impacts on katabatic wind speed are simulated for SST (Figs. S4 and 4c and f) and combined SIC-SST anomalies in summer (Figs. S4 and 4d and g) since summer SIC anomalies do not strongly affect near-surface air temperature. In winter, the combined effects of SIC decrease and SST increase on surface pressure add up to result in slightly stronger katabatic winds (Fig. 5d and g). These results suggest that in a future warmer climate (Fettweis et al., 2013a), the combination of SIC decline and SST increase might strengthen katabatic winds, so as to further weaken the oceanic forcing influence on GrIS SMB.

5 Conclusions

The direct impact of oceanic forcing on GrIS SMB is limited to coastal regions, especially along the western periphery, where SMB is driven by runoff variability, and the southeastern coast, where SMB is driven by precipitation variability. Changes in SIC impact winter snowfall in the south-eastern GrIS by modifying the moisture and heat fluxes between the ocean and the atmosphere. Solid precipitation is enhanced for a SIC reduction, leading to a positive anomaly in GrIS SMB. An increase in SST also enhances evaporation and near-surface warming, leading to a rise in GrIS runoff which exceeds the increase in precipitation. The net result is a negative SMB anomaly. Because of this compensating effect, the combined impact is small. A decrease in SIC, associated with a SST increase, leads to both higher snowfall and runoff, leaving SMB almost unchanged. These results are consistent with previous studies focusing on individual changes in SIC (Day et al., 2013), SST (Hanna et al., 2009), and combined SIC-SST forcings (Hanna et al., 2013a). In contrast, Day et al. (2013) suggest a net decrease in SMB induced by a SIC reduction combined with a SST increase. Because

HadRM3 underestimates contemporary GrIS precipitation and overestimates runoff (Vernon et al., 2013), this compensation effect is less efficient in their study. This highlights the importance of accurately simulating contemporary SMB components, since their response to changes are non-linear because of the feedback between albedo, conditioned by snowfall, and melt.

This study shows that oceanic forcing is very likely not directly involved in the various melt records that were set over the GrIS since 2007. The main reason is that katabatic winds over the ice sheet are strong enough to prevent near-surface oceanic air from penetrating far onto the ice sheet and hence affecting its SMB. At most, oceanic forcing may have contributed to SMB anomalies in coastal regions, where katabatic winds dissipate. In a future warmer climate, a rise in SST associated with a decline in SIC might strengthen Greenland katabatic winds by increasing the thermal contrast between the warmer ocean and the cold interior ice sheet. This could further reduce the direct oceanic impact on GrIS SMB.

The 2007–2012 melt records are more likely associated with the recent persistent negative phase of the NAO, favouring south-westerly winds advecting warm air to the GrIS, resulting in enhanced surface melting. It is possible that oceanic forcing partly caused the recent NAO anomaly (Overland and Wang, 2010; Jaiser et al., 2012). Continued sea ice reduction in summer may thus lead to prolonged phases of negative NAO, further accelerating GrIS surface melt (Jaiser et al., 2012). The Arctic warming amplification, induced partly by the positive melt-albedo feedback, may also be a factor in the negative NAO trend observed since 2007 (Overland and Wang, 2010; Jaiser et al., 2012). Finally, even though oceanic forcing does not directly affect GrIS SMB in a significant way, it does directly impact the calving rate of marine terminating glaciers in the south-east and north-west of Greenland (Thomas et al., 2003; Howat et al., 2005; Luckman and Murray, 2005; Bindschadler, 2006), when warm North Atlantic water infiltrates coastal fjords and melts the bottom of floating glacier tongues (Hanna et al., 2009).

TCD
8, 1453–1477, 2014

Supplementary material related to this article is available online at http://www.the-cryosphere-discuss.net/8/1453/2014/tcd-8-1453-2014-supplement.pdf.

References

Bamber, J. L., Ekholm, S., and Krabill, W. B.: A new, high-resolution digital elevation model of Greenland fully validated with airborne laser altimeter data, J. Geophys. Res., 106, 6733–6745, doi:10.1029/2000JB900365, 2001. 1463

Bamber, J. L., Griggs, J. A., Hurkmans, R. T. W. L., Dowdeswell, J. A., Gogineni, S. P., Howat, I., Mouginot, J., Paden, J., Palmer, S., Rignot, E., and Steinhage, D.: A new bed elevation dataset for Greenland, The Cryosphere, 7, 499–510, doi:10.5194/tc-7-499-2013, 2013. 1458

Bindschadler, R.: Hitting The Ice Sheets Where it Hurts, Science, 311, 1720–1721, doi:10.1126/science.1125226, 2006. 1465

Box, J. E., Bromwich, D. H., and Bai, L. S.: Greenland ice sheet surface mass balance 1991–2000: Application of Polar MM5 mesoscale model and in situ data, J. Geophys. Res., 109, D16105, doi:10.1029/2003JD004451, 2004. 1460

Box, J. E., Fettweis, X., Stroeve, J. C., Tedesco, M., Hall, D. K., and Steffen, K.: Greenland ice sheet albedo feedback: thermodynamics and atmospheric drivers, The Cryosphere, 6, 821–839, doi:10.5194/tc-6-821-2012, 2012. 1456, 1462

Brun, E., David, P., Sudul, M., and Brunot, G.: A numerical model to simulate snow-cover stratigraphy for operational avalanche forecasting, J. Glaciol., 38, 13–22, 1992. 1457, 1458

Day, J. J., Bamber, J. L., and Valdes, P. J.: The Greenland Ice Sheet's surface mass balance in a seasonally sea ice-free Arctic, J. Geophys. Res.-Ea. Surf., 118, 1533–1544, doi:10.1002/jgrf.20112, 2013. 1455, 1456, 1464

Dee, D. P., Uppala, S. M., Simmons, A. J., Berrisford, P., Poli, P., Kobayashi, S., Andrae, U., Balmaseda, M. A., Balsamo, G., Bauer, P., Bechtold, P., Beljaars, A. C. M., van de Berg, L., Bidlot, J., Bormann, N., Delsol, C., Dragani, R., Fuentes, M., Geer, A. J., Haimberger, L., Healy, S. B., Hersbach, H., Hólm, E. V., Isaksen, L., Kållberg, P., Köhler, M., Matricardi, M., McNally, A. P., Monge-Sanz, B. M., Morcrette, J.-J., Park, B.-K., Peubey, C., de Rosnay, P., Tavolato, C., Thépaut, J.-N., and Vitart, F.: The ERA-Interim reanalysis: configuration and

TCD
8, 1453–1477, 2014
Small impact of surrounding oceanic conditions on 2007–2012 GrIS SMB
B. Noël et al.

performance of the data assimilation system, Q. J. Roy. Meteor. Soc., 137, 553–597, doi:10.1002/qj.828, 2011. 1458

de Ridder, K. D. and Gallée, H.: Land Surface-Induced Regional Climate Change in Southern Israel, J. Appl. Meteorol., 37, 1470–1485, doi:10.1175/1520-0450(1998)037<1470:LSIRCC>2.0.CO;2, 1998. 1457

Enderlin, E. M. and Howat, I. M.: Submarine melt rate estimates for floating termini of Greenland outlet glaciers (2000–2010), J. Glaciol., 59, 67–75, doi:10.3189/2013JoG12J049, 2013. 1454

Ettema, J., van den Broeke, M. R., van Meijgaard, E., and van de Berg, W. J.: Climate of the Greenland ice sheet using a high-resolution climate model – Part 2: Near-surface climate and energy balance, The Cryosphere, 4, 529–544, doi:10.5194/tc-4-529-2010, 2010. 1463

Fettweis, X.: Reconstruction of the 1979–2006 Greenland ice sheet surface mass balance using the regional climate model MAR, The Cryosphere, 1, 21–40, doi:10.5194/tc-1-21-2007, 2007. 1457, 1458, 1462

Fettweis, X., Gallée, H., Lefebre, F., and van Ypersele, J.-P.: Greenland surface mass balance simulated by a regional climate model and comparison with satellite-derived data in 1990–1991, Clim. Dynam., 24, 623–640, doi:10.1007/s00382-005-0010-y, 2005. 1458

Fettweis, X., Tedesco, M., van den Broeke, M., and Ettema, J.: Melting trends over the Greenland ice sheet (1958–2009) from spaceborne microwave data and regional climate models, The Cryosphere, 5, 359–375, doi:10.5194/tc-5-359-2011, 2011. 1458

Fettweis, X., Franco, B., Tedesco, M., van Angelen, J. H., Lenaerts, J. T. M., van den Broeke, M. R., and Gallée, H.: Estimating the Greenland ice sheet surface mass balance contribution to future sea level rise using the regional atmospheric climate model MAR, The Cryosphere, 7, 469–489, doi:10.5194/tc-7-469-2013, 2013a. 1458, 1464

Fettweis, X., Hanna, E., Lang, C., Belleflamme, A., Erpicum, M., and Gallée, H.: *Brief communication* "Important role of the mid-tropospheric atmospheric circulation in the recent surface melt increase over the Greenland ice sheet", The Cryosphere, 7, 241–248, doi:10.5194/tc-7-241-2013, 2013b. 1454, 1456, 1458

Franco, B., Fettweis, X., Lang, C., and Erpicum, M.: Impact of spatial resolution on the modelling of the Greenland ice sheet surface mass balance between 1990–2010, using the regional climate model MAR, The Cryosphere, 6, 695–711, doi:10.5194/tc-6-695-2012, 2012. 1458

Gallée, H. and Schayes, G.: Development of a Three-Dimensional Meso-γ Primitive Equation Model: Katabatic Winds Simulation in the Area of Terra Nova Bay, Antarctica, Mon.

Weather Rev., 122, 671–685, doi:10.1175/1520-0493(1994)122<0671:DOATDM>2.0.CO;2, 1994. 1457

Gallée, H., Guyomarc'h, G., and Brun, E.: Impact of snow drift on the Antarctic ice sheet surface mass balance: possible sensitivity to snow-surface properties, Bound.-Lay. Meteorol., 99, 1–19, 2001. 1458

Gallée, H., Peyaud, V., and Goodwin, I.: Simulation of the net snow accumulation along the Wilkes Land transect, Antarctica, with a regional climate model, Ann. Glaciol., 41, 17–22, doi:10.3189/172756405781813230, 2005. 1458

Hanna, E., Cappelen, J., Fettweis, X., Huybrechts, P., Luckman, A., and Ribergaard, M. H.: Hydrologic response of the Greenland ice sheet: the role of oceanographic warming, Hydrol. Process., 23, 7–30, doi:10.1002/hyp.7090, 2009. 1454, 1455, 1456, 1457, 1464, 1465

Hanna, E., Fettweis, X., Mernild, S. H., Cappelen, J., Ribergaard, M. H., Shuman, C. A., Steffen, K., Wood, L., and Mote, T. L.: Atmospheric and oceanic climate forcing of the exceptional Greenland ice sheet surface melt in summer 2012, J. Climatol., doi:10.1002/joc.3743, 2013a. 1455, 1456, 1457, 1464

Hanna, E., Jones, J. M., Cappelen, J., Mernild, S. H., Wood, L., Steffen, K., and Huybrechts, P.: The influence of North Atlantic atmospheric and oceanic forcing effects on 1900–2010 Greenland summer climate and ice melt/runoff, Int. J. Climatol., 33, 862–880, doi:10.1002/joc.3475, 2013b. 1456

Hoskins, B. J. and Hodges, K. I.: New perspectives on the Northern Hemisphere Winter Storm Track, J. Atmos. Sci., 59, 1041–1061, doi:10.1175/1520-0469(2002)059<1041:NPOTNH>2.0.CO;2, 2002. 1456

Howat, I. M., Joughin, I., Tulaczyk, S., and Gogineni, S.: Rapid retreat and acceleration of Helheim Glacier, east Greenland, Geophys. Res. Lett., 32, L22502, doi:10.1029/2005GL024737, 2005. 1465

Jaiser, R., Dethloff, K., Handorf, D., Rinke, A., and Cohen, J.: Impact of sea ice cover changes on the Northern Hemisphere atmospheric winter circulation, Tellus, 64, 11595, doi:10.3402/tellusa.v64i0.11595, 2012. 1456, 1465

Lefebre, F., Gallée, H., van Ypersele, J.-P., and Greuell, W.: Modeling of snow and ice melt at ETH Camp (West Greenland): A study of surface albedo, J. Geophys. Res., 108, 4231, doi:10.1029/2001JD001160, 2003. 1458

Lefebre, F., Fettweis, X., Gallée, H., van Ypersele, J.-P., Marbaix, P., Greuell, W., and Calanca, P.: Evaluation of a high-resolution regional climate simulation over Greenland, Clim. Dynam., 25, 99–116, doi:10.1007/s00382-005-0005-8, 2005. 1458

Lenaerts, J. T. M., van den Broeke, M. R., van Angelen, J. H., van Meijgaard, E., and Déry, S. J.: Drifting snow climate of the Greenland ice sheet: a study with a regional climate model, The Cryosphere, 6, 891–899, doi:10.5194/tc-6-891-2012, 2012. 1458

Luckman, A. and Murray, T.: Seasonal variation in velocity before retreat of Jakobshavn Isbrae, Greenland, Geophys. Res. Lett., 32, L08501, doi:10.1029/2005GL022519, 2005. 1465

Overland, J. E. and Wang, M.: Large-scale atmospheric circulation changes are associated with the recent loss of Arctic sea ice, Tellus, 62, 1–9, doi:10.1111/j.1600-0870.2009.00421.x, 2010. 1456, 1465

Rennermalm, A. K., Smith, L. C., Stroeve, J. C., and Chu, V. W.: Does sea ice influence Greenland ice sheet surface-melt?, Environ. Res. Lett., 4, 024011, doi:10.1088/1748-9326/4/2/024011, 2009. 1463

Rignot, E., Velicogna, I., van den Broeke, M. R., Monaghan, A., and Lenaerts, J. T. M.: Acceleration of the contribution of the Greenland and Antarctic ice, Geophys. Res. Lett., 38, L05503/1 – L05503/5, doi:10.1029/2011GL046583, 2011. 1454

Stark, J. D., Office, E. M., Donlon, C. J., Martin, M. J., and McCulloch, M. E.: OSTIA: An operational, high resolution, real time, global sea surface temperature analysis system, OCEANS 2007 – Europe, 1–4, doi:10.1109/OCEANSE.2007.4302251, conference Publications, 2007. 1458

Tedesco, M. and Fettweis, X.: 21st century projections of surface mass balance changes for major drainage systems of the Greenland ice sheet, Environ. Res. Lett., 7, 045405, doi:10.1088/1748-9326/7/4/045405, 2012. 1458

Tedesco, M., Fettweis, X., Mote, T., Wahr, J., Alexander, P., Box, J. E., and Wouters, B.: Evidence and analysis of 2012 Greenland records from spaceborne observations, a regional climate model and reanalysis data, The Cryosphere, 7, 615–630, doi:10.5194/tc-7-615-2013, 2013. 1455, 1457

Thomas, R. H., Abdalati, W., Frederick, E., Krabill, W. B., Manizade, S., and Steffen, K.: Investigation of surface melting and dynamic thinning on Jakobshavn Isbrae, Greenland, J. Glaciol., 49, 231–239, doi:10.3189/172756503781830764, 2003. 1465

van Angelen, J. H., van den Broeke, M. R., Wouters, B., and Lenaerts, J. T. M.: Contemporary (1960–2012) evolution of the climate and surface mass balance of the Greenland ice sheet, Surv. Geophys., doi:10.1007/s10712-013-9261-z, 2013. 1463
Vernon, C. L., Bamber, J. L., Box, J. E., van den Broeke, M. R., Fettweis, X., Hanna, E., and Huybrechts, P.: Surface mass balance model intercomparison for the Greenland ice sheet, The Cryosphere, 7, 599–614, doi:10.5194/tc-7-599-2013, 2013. 1465
Wouters, B., Bamber, J. L., van den Broeke, M. R., Lenaerts, J. T. M., and Sasgen, I.: Limits in detecting acceleration of ice sheet mass loss due to climate variability, Nat. Geosci., 6, 613–616, doi:10.1038/ngeo1874, 2013. 1454

Table 1. 2012 JJA sea ice extent anomalies for the reference simulation and SIC sensitivity runs over the integration domain relative to ERA-Interim reanalysis (1979–2012). Sea ice extent is computed using only pixels characterized by a SIC > 20 %. The 2012 JJA SST anomaly is also listed for the reference run.

JJA anom 2012	REF	SIC +3	SIC +6	SIC −3	SIC −6
SIC (10^3 km^2)	−635.4	30.4	589.5	−1274.5	−1670.8
SST (°C)	1.2				

Discussion Paper | Discussion Paper | Discussion Paper | Discussion Paper |

TCD

8, 1453–1477, 2014

Small impact of surrounding oceanic conditions on 2007–2012 GrIS SMB

B. Noël et al.

Table 2. Top: annual mean cumulated GrIS SMB ($Gt\,yr^{-1}$) and its components ($Gt\,yr^{-1}$) for the reference run (2007–2012). Bottom: difference in SMB ($Gt\,yr^{-1}$ and %) and its components ($Gt\,yr^{-1}$) between each sensitivity experiment and the reference run over 2007–2012. The last column lists JJA mean cumulated snowfall (Gt/JJA) over the GrIS for the reference run (top) and the anomalies (Gt/JJA) induced by each sensitivity experiment (bottom). Major variable changes are displayed in bold for the most extreme experiments.

Mean ($Gt\,yr^{-1}$)	SMB	SMB %	Snowfall	Rainfall	Runoff	Melting	JJA SF
Reference	237	–	555	28	354	585	117
Anomaly ($Gt\,yr^{-1}$)	SMB	SMB %	Snowfall	Rainfall	Runoff	Melting	JJA SF
SIC +3	−8	−3.4	−7	0	1	1	1
SIC +6	**−15**	**−6.3**	**−16**	−1	−1	−1	2
SIC −3	10	+4.2	9	0	−2	−2	1
SIC −6	**16**	**+6.8**	**13**	0	−3	−4	2
SST −2	8	+3.4	−7	−2	−17	−13	5
SST −4	**15**	**+6.3**	**−12**	**−4**	**−29**	−22	**8**
SST +2	−5	−2.1	17	4	25	23	−4
SST +4	**−13**	**−5.5**	**37**	**9**	**59**	54	**−9**
SIC +3/SST −2	−1	−0.4	−14	−2	−14	−10	4
SIC +6/SST −4	2	+0.8	**−19**	**−4**	**−22**	−15	**7**
SIC −3/SST +2	1	+0.4	23	4	26	24	−4
SIC −6/SST +4	−7	−3	**48**	**10**	**64**	58	**−10**

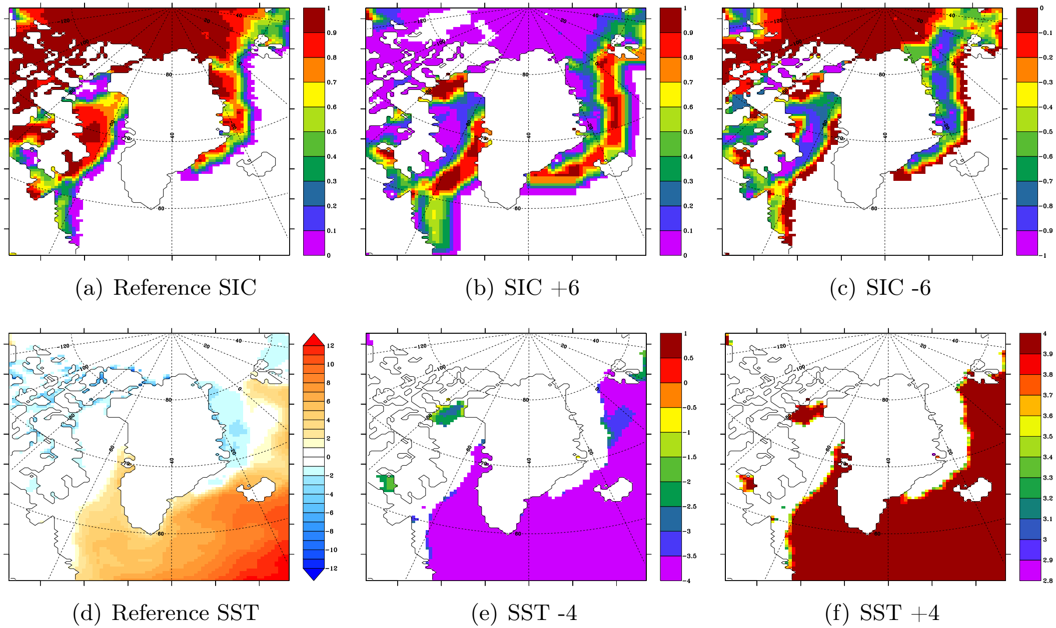

Fig. 1. Top: reference simulation **(a)** SIC and anomalies in SIC from the sensitivity experiment **(b)** SIC +6, **(c)** SIC −6 on the 1 June 2012. Bottom: reference simulation **(d)** SST (°C) and anomalies in SST from the sensitivity experiment **(e)** SST −4, **(f)** SST +4 on the 1 June 2012.

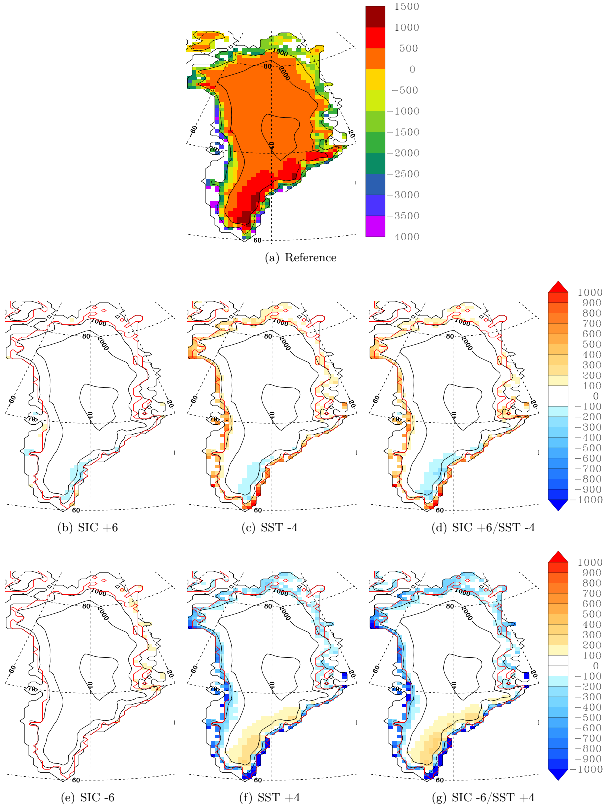

Fig. 2. Annual mean cumulated SMB (mm WE yr^{-1}) for the reference run **(a)**, using the MAR model (2007–2012). Difference in the annual mean cumulated SMB (mm WE yr^{-1}) between **(b)** SIC +6, **(c)** SST −4, **(d)** SIC +6/SST −4, **(e)** SIC −6, **(f)** SST +4, **(g)** SIC −6/SST +4 experiments and the reference run.The red thick line defines the GrIS area in MAR.

TCD
8, 1453–1477, 2014

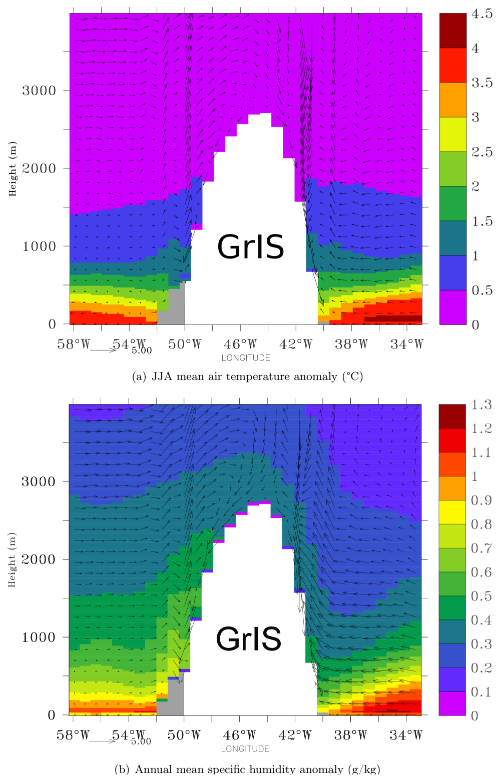

Fig. 3. Longitudinal section trough the GrIS (60° N), showing **(a)** JJA mean wind speed ($\mathrm{m\,s^{-1}}$) for the reference run over 2007–2012, **(b)** same for annual mean. The wind speed can be estimated using the arrow size ($5\,\mathrm{m\,s^{-1}}$) beneath the graphs. The background colours in **(a)** show the difference between JJA mean air temperature (°C) from the SIC −6/SST +4 and the reference run. **(b)** Same for annual mean specific humidity ($\mathrm{g\,kg^{-1}}$). The grey area corresponds to the tundra region surrounding the GrIS.

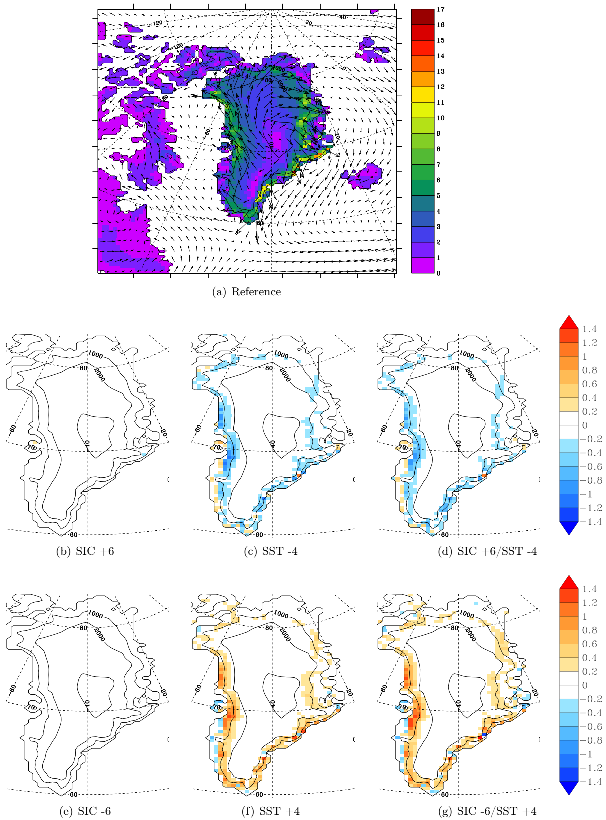

Fig. 4. JJA mean wind speed ($m\,s^{-1}$) for the reference run **(a)** over 2007–2012. Difference in the JJA mean wind speed ($m\,s^{-1}$) between **(b)** SIC +6, **(c)** SST −4, **(d)** SIC +6/SST −4, **(e)** SIC −6, **(f)** SST +4, **(g)** SIC −6/SST +4 experiments and the reference run.

TCD
8, 1453–1477, 2014

TCD
8, 1453–1477, 2014

Title Page
Abstract | Introduction
Conclusions | References
Tables | Figures
◀| |▶
◀ ▶
Back | Close
Full Screen / Esc
Printer-friendly Version
Interactive Discussion

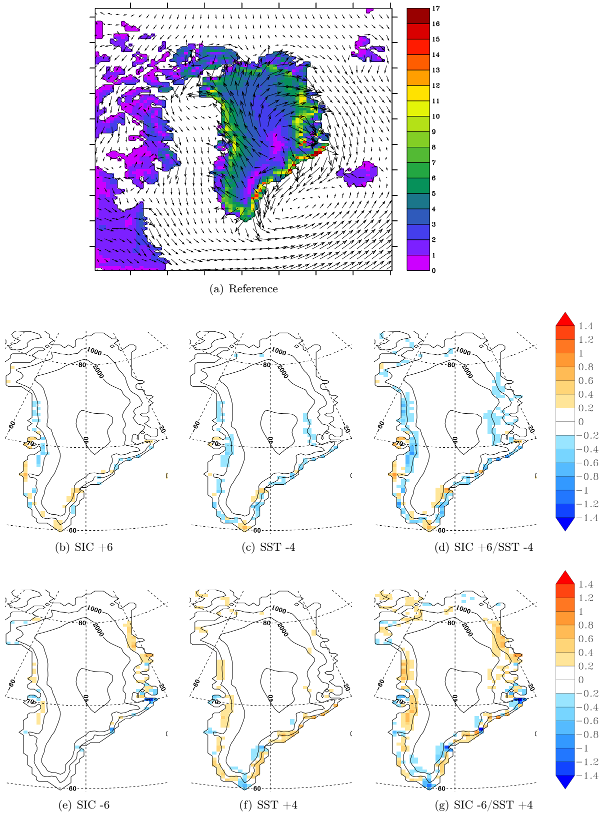

Fig. 5. Annual mean wind speed (m s^{-1}) for the reference run **(a)** over 2007–2012. Difference in the annual mean wind speed (m s^{-1}) between **(b)** SIC +6, **(c)** SST −4, **(d)** SIC +6/SST −4, **(e)** SIC −6, **(f)** SST +4, **(g)** SIC −6/SST +4 experiments and the reference run.